World Scientific
www.worldscientific.com

Application and development of fluorescence probes in MINFLUX nanoscopy (invited paper)

Jing Wang[*,†,‡], Zhen Zhang[*,†], Hongyu Shen[*,†], Qi Wu[*,†] and Min Gu[*,†,§]

Institute of Photonic Chips
University of Shanghai for Science and Technology
Shanghai 200093, P. R. China

†*Centre for Artificial-Intelligence Nanophotonics*
School of Optical-Electrical and Computer Engineering
University of Shanghai for Science and Technology
Shanghai 200093, P. R. China
‡*wangj@usst.edu.cn*
§*gumin@usst.edu.cn*

The MINimal emission FLUXes (MINFLUX) technique in optical microscopy, widely recognized as the next innovative fluorescence microscopy method, claims a spatial resolution of 1–3 nm in both dead and living cells. To make use of the full resolution of the MINFLUX microscope, it is important to select appropriate fluorescence probes and labeling strategies, especially in living-cell imaging. This paper mainly focuses on recent applications and developments of fluorescence probes and the relevant labeling strategy for MINFLUX microscopy. Moreover, we discuss the deficiencies that need to be addressed in the future and a plan for the possible progression of MINFLUX to help investigators who have been involved in or are just starting in the field of super-resolution imaging microscopy with theoretical support.

Keywords: Fluorescence probes; MINFLUX nanoscopy; photoblinking; super-resolution imaging; labeling strategy.

1. Introduction

Microscopy has long been recognized as one of the most valuable and rapidly evolving research techniques, with numerous biological milestones coinciding with the development of newer, more powerful microscopes. Nonetheless, similar to any other optical system, the spatial resolution (SR) of fluorescence microscopy (FM) is confined by the diffraction limit, which was first recognized at the end of the 19th century by Ernst Abbe.[1] Several processes commonly known as "super-resolution microscopy" have exceeded this diffraction restriction in recent decades. Among them are stimulated emission depletion (STED)/reversible saturable

optical linear fluorescence transitions (RESOLFT) microscopy[2,3] and photoactivated localization microscopy (PALM)/stochastic optical reconstruction microscopy (STORM),[4–6] which typically achieve resolutions on the lateral in the 20–50 nm range,[7–9] with the fluorophore photostability acting as a constraint. Resolution in the axial direction is typically 2- to 3-fold worse in the 60–120 nm range.

The newly introduced MINimal emission FLUXes (MINFLUX) technique has further pushed the SR down to a few nanometers,[10] which takes advantage of coordinate targeting for single-molecule localization. Although MINFLUX is still in its early stages as far as applications are concerned, it has demonstrated the ability to characterize subcellular structures with nanometer resolution and to discover supramolecular protein structures.[11–13] However, the maximum capabilities of MINFLUX have yet to be realized, particularly in the imaging of living cells. Obtaining such high-accuracy data necessitates more than just having access to microscopes with high resolution. It also relies on detecting molecules and the properties that are generally linked to them. It is essential that the evaluated signals generated by fluorophores are completely tagged and distance away from the target molecules.

Particular care must be taken to the sample preparation, including selecting fluorescent molecules and corresponding labeling methods appropriate for the selected super-resolution microscopy approach. Furthermore, a solid understanding of the employed procedure is required to account for potential issues throughout acquiring and processing, and to properly scale up experimental studies to collect large datasets for robust quantitative measurements. As a result, the primary goal of this article is to review the use of multiple organic fluorophores in MINFLUX, as well as their effectiveness in exploring subcellular organelles by exceeding the diffraction constraint. Another purpose is to attempt to provide eligibility requirements for excellent fluorescent probes and labeling methods to select or produce for future MINFLUX-based improved learning.

2. Technical Principles of MINFLUX

2.1. *The basic concept of MINFLUX*

In terms of superresolution FM (nanoscopy) concepts,[14,15] MINFLUX imaging is notable for its ability to achieve molecular-scale precision regularly.[10,11] The fluorophores in MINFLUX imaging switch separately, as in PALM/STORM imaging,[16–19] while the localization is completed with a structured (doughnut-shaped) higher specific beam zero point as close to the molecule as possible. Preferably, the nearer this zero is to the fluorophore, the weaker the fluorescence emitted will be and fluorescence will stop when the zero placement corresponds accurately with the location of the fluorophore. So in MINFLUX the emitter position is determined not by the presence of fluorescence, but by where it is not present. MINFLUX achieves the nanosized higher accuracy with a relatively small number of identified photons, N, than centroid-based localization. It should be noted that a single emission (for example, because of a minor misusage) might be sufficient to indicate that the molecule is not at the place of the doughnut zero.

Unluckily, we cannot precisely position the doughnut zero at the small molecules control point in a single image. However, this Gedanken investigation indicates that approaching the molecular position by targeting the zero of the excitation doughnut to the molecule must decrease the number of identified photons necessary for localization. This is because the placement of the doughnut zero is well known, and the subsequent fluorescence suggests the molecule's remaining space to the zero. As a result, in addition to verifying the molecule's existence, the generated fluorescence contains information about the molecule's position.[10] Fluorescence is the result of the mismatch between the molecular location and the zero's position, which indicates that the tinier the mismatch, the fewer are the fluorescence photons required for localization. For this reason, in the implementation of MINFLUX,[20,21] the molecule's location is investigated with the driven beam scans around the preset location of the fluorophore. The number of observed photons is used to determine location. (Figs. 1(a) and 1(b)).[10]

Specifically, a laser beam with zero central intensity was used as excitation, which was in the shape of a horizontal doughnut at 2 D MINFLUX (Fig. 1(c)) and a hollow sphere in space (bottle-beam) at 3D MINFLUX (Fig. 1(d)). Based on the predicted zero intensity position, the known excitation beam shape, and the number of photons released by the fluorescent molecule at different positions of the excitation beam, the fluorescent
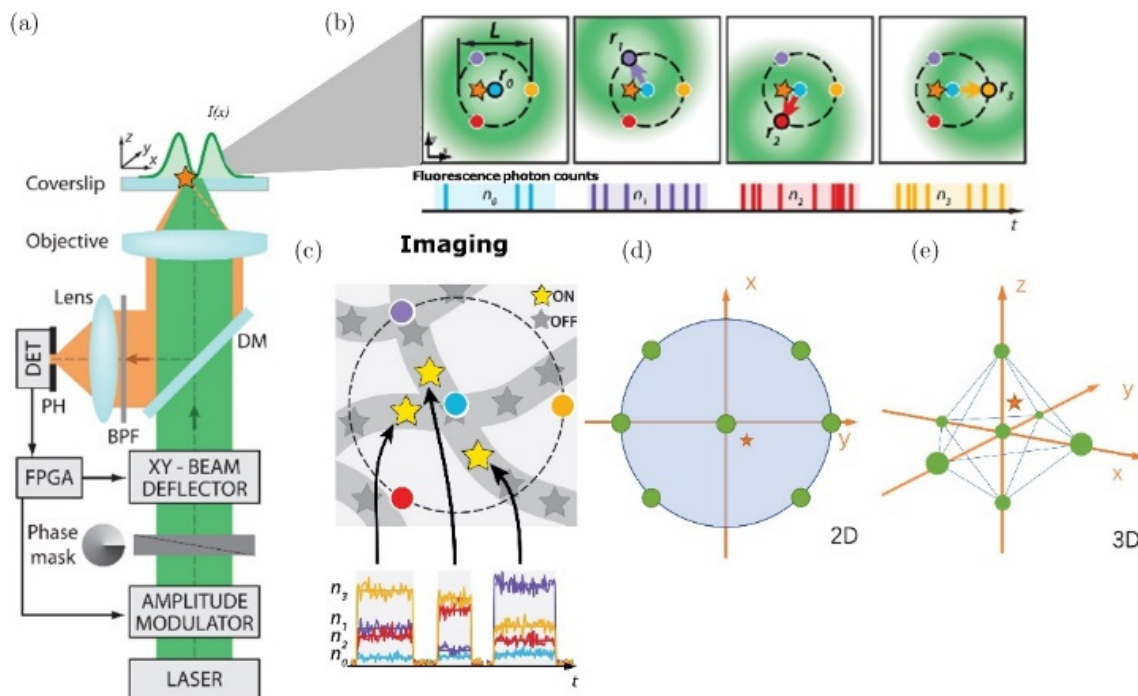
Fig. 1.   The MINFLUX concept. (a) Scanning fluorescent microscope with confocal identification and a donut-shaped excitation beam. (b) At 04 different sites, an emitter (star) is sequentially subjected to the excitation beam, trying to collect distinct fluorescence signals. (c) By sequentially localizing blinking molecules, the concept can be applied to imaging. (d) 2D MINFLUX uses a hexagonal pattern with a central point as the preset detection position for the donut excitation beam. (e) In 3D MINFLUX, the exciting light spot is a 3D donut, a hollow sphere, and an octahedron preset detection position constitute the beam detection mode.

molecule can be precisely located after several iterations. In each iteration process, the doughnut-shaped excitation beam is centered on the localization of the latest fluorophore. The diameter L of the doughnut movement is gradually reduced to improve the resolution further. During the whole iteration process, the location information of each detected fluorescence molecule will be accumulated into the information for the next detection. In contrast, traditional super-resolution methods always detect all photons in the same way, each time obtaining the same low amount of information as the first photon.

Compared with the classical single-molecule localization microscopy (SMLM) technology, the MINFLUX technology can use less than 1,000 photons and a lower light dose to achieve localization accuracy at the molecular scale. MINFLUX localization does not have to wait for huge numbers of fluorescence photons, and it makes each emitted photon more instructive. As a consequence, this nm size localization is significantly quicker than the "passive" camera-based localization in PALM/STORM.

2.2.   *Technical development of MINFLUX*

Along with the basic MINFLUX imaging methods listed above, many other MINFLUX imaging methods have been reported, each of which has significantly contributed to the advancement of MINFLUX microscopy. In Ref. 22, Luciano A. Masullo and co-authors introduced pulsed interleaved MINFLUX (p-MINFLUX). p-MINFLUX is a new version of the extremely photon-efficient single-molecule localization process which involves fluorescence lifetime information. Unlike the original MINFLUX implementation, p-MINFLUX employs interleaved laser pulses to distribute the doughnut-shaped excitation foci at the highest possible repetition rate. p-MINFLUX nanoscopy indicated localization exactness of $\sigma \approx 1$–2 nm with $N \approx 1000$ photons per localization. Furthermore, p-MINFLUX is distinct in that it gives a link to energized lifetime data, allowing for single-molecule identification (multiplexing) and FLIM nanoscopy with molecular-scale resolution (Fig. 2); which is a 10–100 times advancement over earlier works.[23,24]
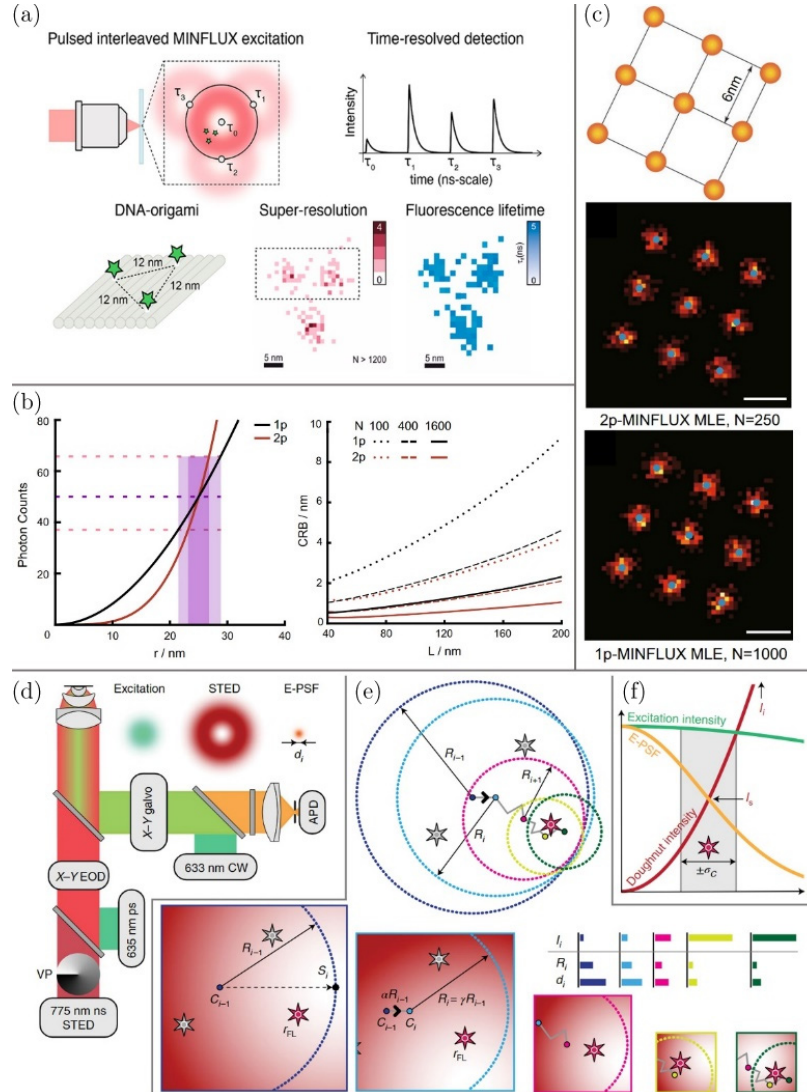
Fig. 2. (a) The p-MINFLUX concept: 4 pulsed interpolated doughnut-shaped signals are concentrated on the specimen in a triangular pattern, with the 4th beam positioned in the triangle's center. Each pulse's arrival time is represented as τ_i. The positions of fluorescent molecules are indicated by stars. The picture showed the 2D localization image and the p-MINFLUX fluorescence lifetime image for one DNA origami structure. (b) Comparison of localization precision and Cramér-Rao Bound (CBR) with respect to N and L, between single-photon and two-photon MINFLUX. (c) Imitation on the origami of 2p-MINFLUX and1p-MINFLUX. Principles of MINSTED localization: (d) Schematic representation of the MINSTED setup. In the focal plane, a 633 nm CW laser beam was used for fluorophore pre-identification. An electro-optical deflector directs the co-aligned pulsed lasers for excitation and STED at 635 and 775 nm in the focal plane of the objective lens (EOD). For helical phase modulation, a vortex phase plate (VP) was used to shape the STED beam into a doughnut; (e) Circular X–Y scans were used to locate the active fluorophore (red among grey stars) at unidentified position rFL. Only Ci is modified when a minimum radius $R_{\min}$ (yellow) is achieved, and the localization ends when the fluorophore becomes inactivated (N detections). The column diagrams show how R_i and d_i minimize as doughnut intensity I_i increases.(F) Normalized probability of excitation (green) and fluorescence detection (E-PSF, yellow) as a function of radial distance ρ from the focal point, along with a non-normalized intensity profile of the STED beam doughnut (red). although I_i is constantly increased during the localization to sharpen the E-PSF, the intensity experienced by the fluorophore remains about Is within the $\pm\sigma C$ position range of the center positions C_i highlighted in grey.

More recently, Zhao **et al.** presented a 02-photon MINFLUX conceptual framework (2p-MIN-FLUX).[25] Their simulation studies show that the square of fluorescence intensity results in a 2-fold rise in the highest localization accuracy over 1p-MINFLUX. As shown in Fig. 2(b), when comparing with 1p-MINFLUX with $N = 1000$, 2p-MINFLUX with $N = 250$ achieves comparable

localization distributions, verifying 2p-ability MINFLUX's to decrease the number of photons needed. Following the MINFLUX enabled molecular precision, a similar resolution is obtained in MINSTED nanoscopy.[26,27] Specifically, in nanoscopy of MINSTED, just one fluorophore is activated at a time inside a diffraction-limited zone. Like MINFLUX, MINSTED also uses the STED doughnut's intensity least as a moving reference collaborative for fluorophore localization. The relatively closer it is to the fluorophore, the lesser the likelihood of STED and the higher the likelihood of fluorescent emission. Compared to the related concept of MINFLUX, looking for the doughnut position with the least STED is equivalent to looking for the position with the most fluorescence.

3. The Application of MINFLUX Nanoscopy Imaging

Thus far, MINFLUX imaging has been performed on NPCs,[10] MICOS proteins in mitochondria,[13] axonal bII spectrin in primary hippocampal neurons,[12] and several kinds of presynaptic Active Zone.[28] To continue pursuing effective bio-imaging, the emission and excitation wavelength ranges of the selected fluorophore must match those of the given microscopic system. MINFLUX imaging has been successfully deployed in several dyes, such as Alexa Fluor 647, CF660C, and CF680. They are all around its typical excitation wavelength of 642 nm (Table 1). For instance, Roman Schmidt *et al.*[12] resolved the symmetry of Nup96, a protein from the nuclear pore complex (NPC) (Figs. 3(a)–3(d)), dispersed along a 110 nm diameter ring, in line with previous initial results.[11] The localizations generally constructed 8 clusters, each of which contains 2 to 4 subclusters, representing the sum of Gaussian distributions, one for every localization, showing personal Nup96 proteins via their specific fluorescent markers.[29] Roman Schmidt *et al.*[12] also used MINFLUX to visualize immunolabeled spectrin in the extremely periodic actin–spectrin protein lattice of a rat axon (Fig. 3(f)) and the PMP70 protein on the surface of peroxisomes (Fig. 3(g)) in Vero cells. Gwosch *et al.*[11] confirmed the distribution of Mic60 clusters in two narrow opposite bands along the mitochondrion of a Mic10-KO cell (Fig. 3(e)), which is entirely different to their stripe-like distribution in WT cells.[30]

The random blinking guarantees that fluorophores are distributed sparsely, and the high contrast enables us to record MINFLUX images of densely labeled microstructures. Currently, a random conversion similar to STORM[4,31] was used to switch the fluorophore between fluorescent and dark states by combining organic dyes with buffer solution. The reducing agent mercaptan in the buffer can be combined with the dye to convert the fluorophore to a dark state. The transition to a fluorescent state can occur spontaneously or be induced by ultraviolet light. Hypoxia can reduce bleaching and spontaneous scintillation of dyes so that the fluorescence scintillation can be controlled by ultraviolet light. The photophysical properties of traditional fluorophores are strongly environment-(buffer)-dependent, limiting their use for super-resolution imaging to particular environments and only for fixed cell imaging.

In 2020, for the first time, Gwosch *et al.* achieved nanometer resolution in biological specimens from living cells with the photo-converting fluorescent protein mMaple.[11] In order to better use MINFLUX to study dynamic problems, probes that can be used in living cells need to be further developed.

Table 1. Summary of the fluorophores used in MINFLUX imaging.

Fluorophore	λ_{ex} (nm)	λ_{em} (nm)	$\lambda_{on/off}$ (nm)	$\varepsilon(\mathrm{M}^{-1} * \mathrm{cm}^{-1})$	References
Alexa Fluor647	650	665	405/642	239000	10–12
Atto647N	646	664	405/642	150000	12, 13
CF660c	667	685	405/642		11
CF680c	681	698	405/642	210000	11
Hydroxymethyl Silicon-rhodamine (HMSiR)	650	671	self-blinking		36
Photoactivatable Xanthones (PaX)	560	598	405/560	66000	37

Notes: λ_{ex}, the wavelength of excitation; λ_{em}, a wavelength of emission; $\lambda_{on/off}$, wavelengths for turning on and off fluorescence, correspondingly; ε, coefficient of extinction.
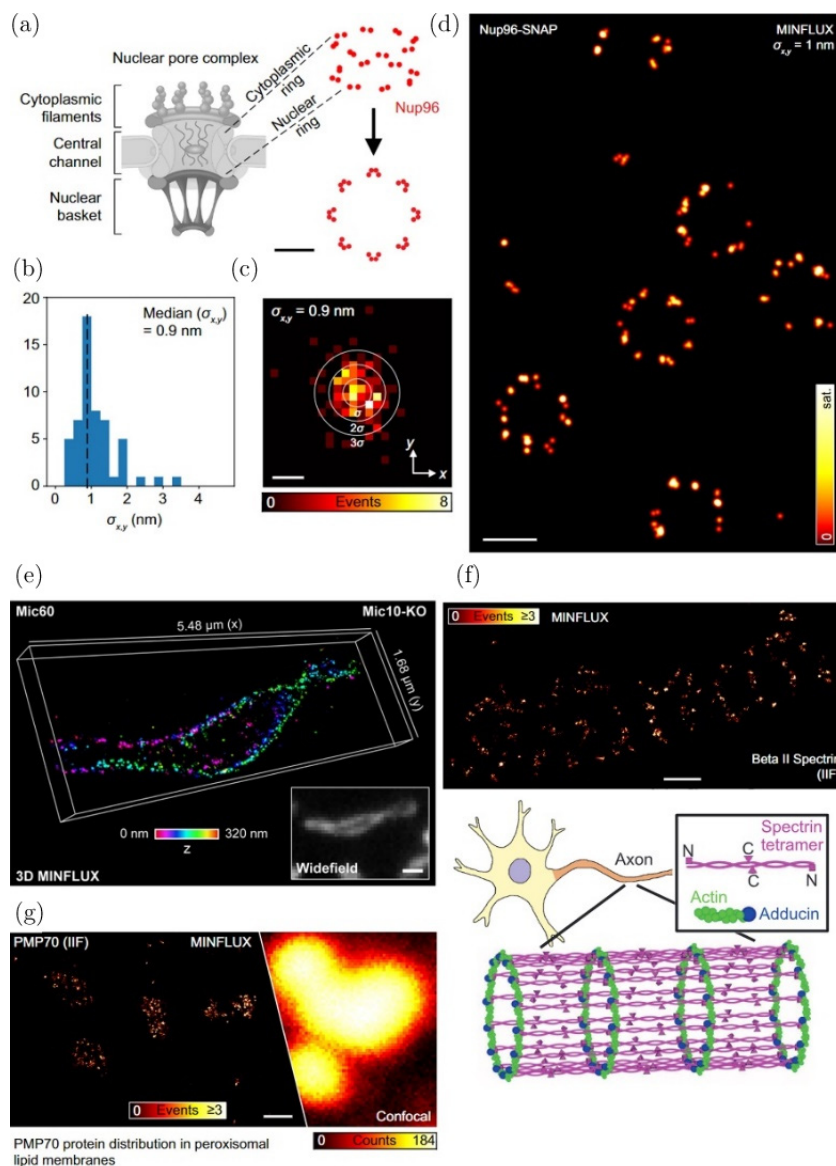
Fig. 3. Nanometric highly precise fluorescence imaging of labeled cellular ultrastructure using MINFLUX. (a) Nup96 localizes in two eightfold-symmetric rings within the nuclear pore complex. (b) Histogram of the standard deviation from sets of sequential localizations based on 2100 photons each taken from the uninterrupted photon emission traces at the final MINFLUX iteration step. (c) Histogram of the distance of a localization to the mean position of a single fluorophore (data as in (b)). The ellipses are displayed with semi-axes of σ, 2σ, and 3σ in length, with σ the precision obtained from a combined analysis of the statistical localization spread (standard deviation) in x and y. (d) MINFLUX nanoscopy reconstruction of Nup96-SNAP labeled with Alexa Fluor 647. (e) 3D MINFLUX nanoscopy. Mic10-KO cells were immunolabeled for Mic60 using a directly labeled antibody. Colors encode depth information. (f) BetaII spectrum from hippocampal neuron axon of rat. (g) PMP70 in Vero cell peroxisomes. A confocal scan of peroxisomes found nearby is included for comparison. Scale bars; 50 nm (a), 2 nm (c), 100 nm (d), 200 nm (f, g).

4. Future Perspectives of Fluorescent Probes Development for MINFLUX

MINFLUX has allowed biologists to visualize structures of the cells with molecular exactness, providing unique insights into the sizes, quantities, as well as spatial proportions of macromolecules within the cell. High-quality super-resolution imaging requires high photophysical and chemical characteristics of fluorescent analyses. Suffice it to say, the choice of appropriate fluorophore must satisfy some crucial characteristics to possibly be used in MINFLUX imaging. In this segment, we describe the unique properties of fluorescent probes in MINFLUX imaging, focusing on the deficiencies

of traditional sample preparation methods and the importance of optimal labeling of molecular targets.

4.1.   *Spontaneous blinking probes*

In the localization mode, MINFLUX microscopy uses blinking fluorophores, or switches on and off probabilistically. Generally, to cause the fluorophore to switch on and off, powerful laser beam and additives, for example, thiols (10–100 mM) in shape referred to as blinking buffers are required, restricting live-cell applications of this technique. Moreover, for traditional redox-active blinking buffer probes, the image processing buffer components must be carefully optimized for every fluorophore. As a result, finding optimum conditions that stimulate the blinking of various fluorophores to visualize two distinct targets simultaneously is especially difficult. Fluorophores that instantaneously blink and can switch on/off probabilistically without using a high-powered laser or any additives (Fig. 4(a))[32,33] are more suitable for multicolor and live-cell MINFLUX imaging. For example, Urano[20] established silicon-rhodamines dyes with an appending inner nucleophilic attack at the 2-position, such as HMSiR. Comparable to 2′-carboxyrhodamines, they generally create a nonfluorescent spirocyclic pattern in thermodynamic equilibrium with their fluorescent form in the ground state (Figs. 4(b) and 4(c)).[34,35] Ruta Gerasimaite *et al.* have successfully used it for Tubulin-targeted MINFLUX imaging (Figs. 4(d)–4(g)).[36] Very recently, Richard Lincoln *et al.* developed a new kind of photoactivatable xanthones (PaX) dyes which can be used in live-cell labeling for MINFLUX nanoscopy imaging.[37] In addition to organic molecules, several nanomaterials also have a random blinking effect, which is expected to be used in MINFLUX imaging in the future.[38–41]

4.2.   *Ultra-small size probes*

It is essential to mention that the evaluated signals are generated by fluorophores separated by a full tag length of the desired molecules. If the labels are greater than the method's resolution, any assumption of molecule position cannot be completely accurate. Therefore, we should carefully choose fluorophores and a proper labeling strategy. Affinity-based labeling is arguably the most adaptable

and extensively used method in all fluorescence microscopy applications.[42,43] However, a usual primary and secondary antibody combination is frequently quite large; as a result, the effective resolution is limited in MINFLUX nanoscopy imaging. Its disadvantage is background due to nonspecific staining.[44] Another commonly used label is the appearance of fluorescent protein (FP) fusions to study target distribution within the cells.[45] FPs covalently bind the cellular proteins through targeted genetic modifications.[46] It has the apparent benefit of allowing for live-cell imaging. However, this method is used to obtain unmarked proteins, which are not observed in fluorescent assessments.[47] Instead of appearing as an FP, desired proteins can be hereditarily attached to a scaffold that entangles free fluorescence substances in solution. This is the main method for MINFLUX imaging.[10–13] SNAP proteins are very widely used "self-labeling" proteins.[48] Moreover, HaLo[49] labels, can be responded covalently with the molecules chloralkane (CA) and benzylguanine (BG), correspondingly. The primary benefit is that these substances are attached to organic dyes, which are frequently shiner, more photostable, and much more varied than FPs. Smaller probes virtually eliminate this size problem, such as nanobodies,[50] which are predicted to play a substantial role in MINFLUX imaging. In Table 2, we assess the most commonly used strategies.

4.3.   *High contrast ratio and low duty cycle*

In principle, one of the most crucial aspects for obtaining a high-resolution imaging is to reduce the background signal. The background in MINFLUX nanoscopy can be caused by the auto-fluorescence of the reagents or by the fluorophores. A fluorophore with photoswitchability, for example, is predicted to switch between the fluorescent "on" and "off" states, with the fluorophore preferably not emitting any photons in the "off" state. Moreover, the fluorescent "off" state does not always indicate zero photon output. Triplet fluorescent probes, for instance, can discharge weakly and contribute to the background even though they lack significant emission profiles. As a result, the organic dyes selected for MINFLUX must emit as few photons as feasible in the "off" state and have a better contrast ratio. Another factor to consider when choosing
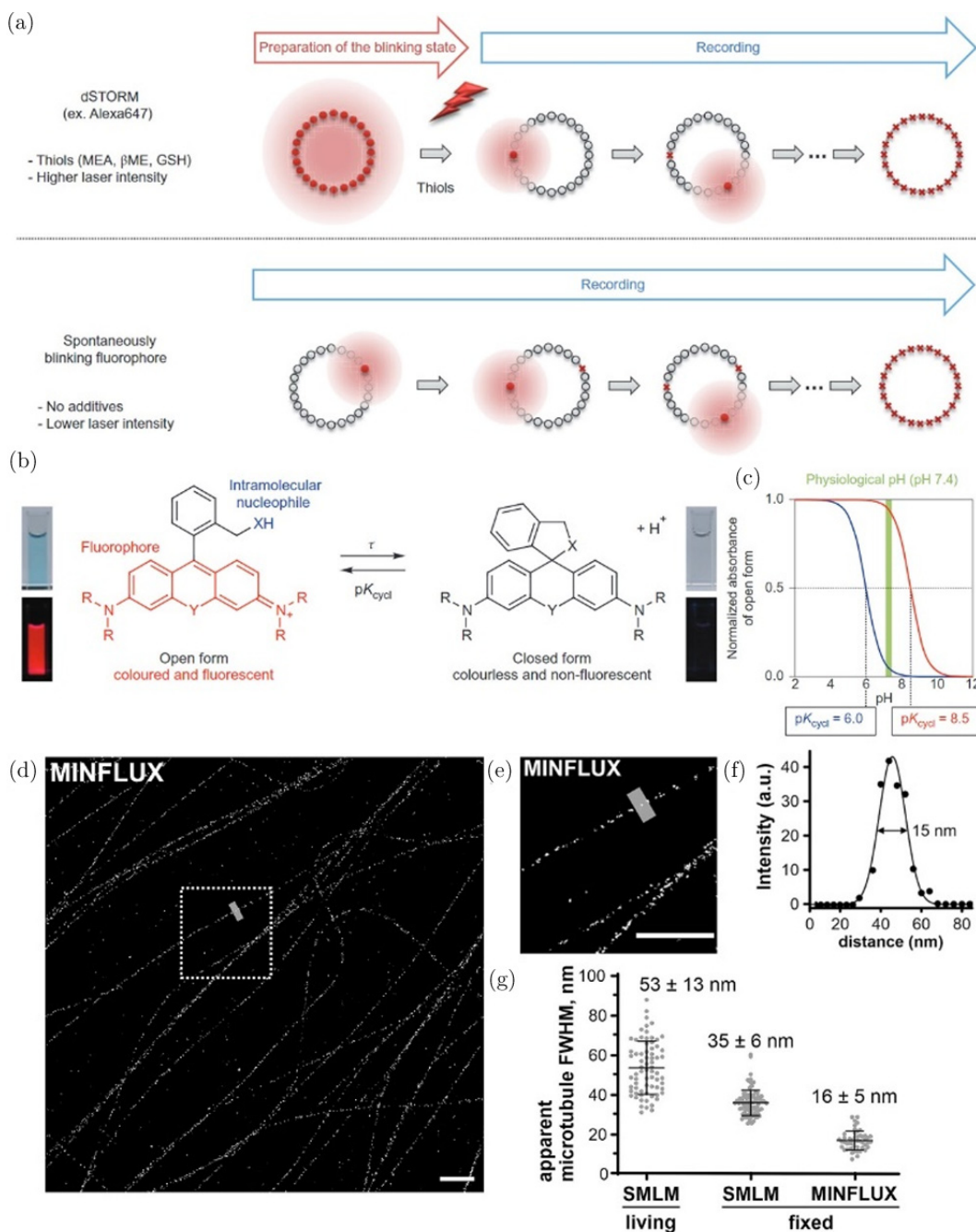
Fig. 4. (a) A traditional fluorophore and an instantaneously blinking fluorophore were used in a single molecule localization pattern. (b) Intramolecular spirocyclization thermal equilibrium between non-fluorescent closed-form and fluorescent open form. The equilibrium constant for intra-molecular spirocyclization is pKcycl, and the entire life of the open form is (the time it takes for the open form to switch back to the closed-form). (c) Representative pH titration curves of rhodamine derivatives with pKcycls of 8.5 (red) and 6.0 (blue). (d) Image of microtubules in specified U-2 OS cells colored with HMSiR tubulin using MINFLUX. 500 nm scale bar. (e, f) The inset shows a profile of the line zone (200 nm in width). (g) SMLM and MINFLUX nanoscopy were used to evaluate microtubule fwhm.

probes for MINFLUX image analysis is the duty cycle. When a fluorophore is excited at a specific wavelength, it gives off fluorescence, referred to as the fluorescence "on" state, while the nonemitting state is referred to as the fluorescence "off" state. The duty cycle is determined as the percentage of time being spent in the "on" state to time being spent in the "off" state for a fluorophore.[51]

Table 2.   Comparison of potential labeling strategies used in MINFLUX nanoscopy.

	Label	Ref	Size	Description	Characteristics
Affinity binding	Antibody IgG or Fab fragment	42, 43	∼12 nm/150 kDa	IgG: antigen-specific Immunoglobulin G antibodies with 02 similar massive chains and 02 identical light chains light chained together in a Y-shape. Fab: Antigen-specific monovalent pieces of IgG and IgM made up of changeable light and heavy chain zones linked by disulfide bonds.	Classic immunofluorescence by primary and secondary antibody Combination Ctotal length: 20–30 nm Large tags limit the image resolution. Not cell-permeable, thus, limiting live-cell staining as a specialized delivery method is needed.
	Nanobody	50	∼3 nm/∼15 kDa	Single antigen-specific variable single-chain domain (VHH)Nanomolar affinity antibody	Anti-GFP nanobody is a popular stain. Live-cell stain results in a nonspecific background due to lack of washing.
Genetic fusions	SNAP	48	∼3 nm/∼20 kDa	Ligand binding genetic fusionenzyme to a target protein.	Large selection of ligands coupled to various fluorophores.
	HALO	49	∼30 kDa		Genetic fusion may interfere with protein localization and function. Live-cell staining is only possible for cell- permeable fluorophores or specialized delivery methods.
	Fluorescent proteins	45	∼3 nm/∼25 kDa	Fluorophore genetic fusion to a protein of interest	Live-cell imaging. No need for a staining step in adding external fluorophores during the sample preparation. Highly specific tag. Genetic fusion may interfere with protein localization and function. Factors like maturation time or misfolding must be taken into account. Some fluorescent proteins tend to artificially aggregate for concentrations above a certain threshold.

Therefore, a fluorescent molecule with an extreme duty cycle remains in the fluorescence "on" state for a prolonged duration of time, while a molecule with a low-duty cycle consumes very little time in the "on" state and spends a large part of its time in the "off" state. For MINFLUX image analysis, very few of the fluorophores must emit simultaneously. In contrast, the majority of the fluorophores stay "off" so that the likelihood of two compounds having existed at the same time under the diffraction limit is reduced. Fluorophores with a limited duty cycle are thus advantageous in this regard.

4.4.   *Brightness and photostability*

The photophysical and chemical characteristics of fluorescent probe are also essential for MINFLUX imaging. The final resolution of MINFLUX

microscopy can be presented as $\sigma_{\mathrm{CRB}}(\bar{r} = \bar{0}) = L/2\sqrt{2N}$ (σ_{CRB}: the localization precision of MINFLUX nanoscopy; $\bar{r}$: vector of the donut's position; L: the diameter of targeted coordinate pattern circle; N: the number of detected photons).[10] Elevated
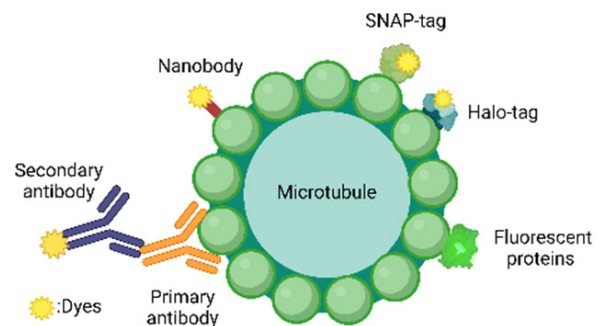

Fig. 5.   A schematic diagram of several labeling strategies in Table 2 (figure was created with Biorender.com).

ultra-resolution microscopy cannot be accomplished without using an appropriate fluorophore. The illumination of the molecules displays the proportion of visible photons, which has a significant effect on the accuracy of the localization. The photostability of substances under constant laser illumination seems to be the most significant factor influencing image quality from a photochemical standpoint. Only fluorophores capable of switching for hundreds or thousands of cycles are suitable for MINFLUX. As a consequence, it is critical to fully understand these photophysical and chemical aspects to better comprehend the context for selecting optimal fluorophores for MINFLUX. The brightness of a particular fluorogenic system is determined by two significant aspects: (a) the coefficient of extinction, and (b) the quantum yield of fluorescence.[52] In the overwhelming bulk of fixed cell MINFLUX research, the fluorophore of choice is Alexa Fluor 647 because of its good photon yields and robust photoswitching. Unfortunately, the fluorophore of Alexa Fluor 647 requires buffer assistance for blinking and cannot be used for living cell MINFLUX imaging. Undoubtedly, live-cell imaging will reveal extra nanoscopic information about living biological systems.

Creating biocompatible fluorophores with small molecules that enable optimized imaging situations is critical for enabling live samples imaging with limited invasiveness.

5. Conclusion and Future Perspectives

The recently introduced MINFLUX nanoscopy method has been very influential. However, its capabilities have several limitations. The most significant constraint preventing further advancement is the scarcity of appropriate probes. In this paper, we have illustrated the latest improvements in MINFLUX-based super-resolution imaging applications using organic fluorescent probes for small molecules. We have also briefly discussed the selection of fluorophores appropriate for effective MINFLUX imaging. The key criteria for selecting and developing new organic fluorescent probes for MINFLUX have been highlighted. With the continued development of MINFLUX-based image processing technology and new labeling techniques in the coming years, the utility of this imaging strategy will certainly be improved. It is necessary to

envisage the sub-diffraction resolution in sub-cellular organelles using live-cell MINFLUX microscopy, which could potentially open a new window for attempting to resolve biologically derived illnesses related to dysfunctions in cells. Because the selection of appropriate fluorophores is the most significant component in obtaining a successful picture of excellent quality, it can be expected that great efforts will be made to build new fluorophores that are flexible with remarkable characteristics for the advancement of imaging reliability.

Acknowledgments

Conflicts of Interest

The authors declare no conflicts of interest relevant to this article.

References

1. E. Abbe, "Beitrage zur Theorie des Mikroskops und der mikroskopischen Wahrnehmung," *Arch. Mikrosk. Anat* **9**(1), 413–468 (1873).

2. S. W. Hell, J. Wichmann, "Breaking the diffraction resolution limit by stimulated emission: Stimulated-emission-depletion fluorescence microscopy," *Opt. Lett.* **19**(11), 780–782 (1994).

3. T. A. Klar, S. Jakobs, M. Dyba *et al.*, "Fluorescence microscopy with diffraction resolution barrier broken by stimulated emission," *Proc. Natl. Acad. Sci. USA* **97**(15), 8206–8210 (2000).

4. M. J. Rust, M. Bates, X. Zhuang, "Sub-diffraction-limit imaging by stochastic optical reconstruction microscopy (STORM)," *Nat. Methods* **3**(10), 793–795 (2006).

5. E. Betzig, G. H. Patterson, R. Sougrat *et al.*, "Imaging intracellular fluorescent proteins at nanometer resolution," *Science* **313**(5793), 1642–1645 (2006).

6. S. T. Hess, T. P. K. Girirajan, M. D. Mason, "Ultra-high resolution imaging by fluorescence photo-activation localization microscopy," *Biophys. J.* **91**(11), 4258–4272 (2006).

7. K. Xu, G. Zhong, X. Zhuang, "Actin, spectrin, and associated proteins form a periodic cytoskeletal structure in axons," *Science* **339**(6118), 452–456 (2013).

8. E. D'Este, K. Dirk, V. Caroline *et al.*, "Subcortical cytoskeleton periodicity throughout the nervous system," *Sci. Rep.* **6**, 22741 (2016).

9. S. J. Sahl, S. W. Hell, S. Jakobs, "Fluorescence nanoscopy in cell biology," *Nat. Rev. Mol. Cell. Biol.* **18**(11), 685–701 (2017).

10. F. Balzarotti, Y. Eilers, K. C. Gwosch *et al.*, "Nanometer resolution imaging and tracking of fluorescent molecules with minimal photon fluxes," *Science* **355**(6325), 606–612 (2017).

11. K. C. Gwosch, J. K. Pape, F. Balzarotti *et al.*, "Minflux nanoscopy delivers 3D multicolor nanometer resolution in cells," *Nat. Methods* **17**(2), 217–224 (2020).

12. R. Schmidt, T. Weihs, C. A. Wurm *et al.*, "MINFLUX nanometer-scale 3D imaging and microsecond-range tracking on a common fluorescence microscope," *Nat. Commun.* **12**(1), 1478 (2021).

13. J. K. Pape, T. Stephan, F. Balzarotti *et al.*, "Multicolor 3D MINFLUX nanoscopy of mitochondrial MICOS proteins," *Proc. Natl. A Sci.* **117**(34), 20607–20614 (2020).

14. S. W. Hell, "Far-field optical nanoscopy," *Science* **316**, 1153–1158 (2007).

15. S. W. Hell, "Nobel lecture: Nanoscopy with freely propagating light," *Rev. Mod. Phys.* **87**, 1169–1181 (2015).

16. D. T. Burnette, P. Sengupta, Y. Dai *et al.*, "Bleaching/blinking assisted localization microscopy for superresolution imaging using standard fluorescent molecules," *Proc. Natl. Acad. Sci. USA* **108**(52), 21081–21086 (2011).

17. S. J. Holden, S. Uphoff, A. N. Kapanidis, "DAOSTORM: An algorithm for high-density super-resolution microscopy," *Nat. Methods* **8**(4), 279–280 (2011).

18. B. Huang, W. Wang, M. Bates *et al.*, "Three-dimensional super-resolution imaging by stochastic optical reconstruction microscopy," *Science* **319**(5864), 810–813 (2008).

19. M. Bates, B. Huang, G. T. Dempsey *et al.*, "Multicolor super-resolution imaging with photo-switchable fluorescent probes," *Science* **317**(5845), 1749–1753 (2007).

20. S. W. Hell, "Method of and apparatus for tracking a particle, particularly a single molecule, in a sample, Patent application WO 2013/072273 A1 B2, 2013.

21. S. W. Hell, High-resolution fluorescence microscopy with a structured excitation beam. Patent application WO 2015/097000 A1, 2015.

22. L. A. Masullo, F. Steiner, J. Zhringer *et al.*, "Pulsed interleaved MINFLUX," *Nano Lett.* **21**, 840–846 (2020).

23. J. C. Thiele, D. A. Helmerich, N. Oleksiievets *et al.*, "Confocal fluorescence-lifetime single-molecule localization microscopy," *ACS Nano* **14**(10), 14190–14200 (2020).

24. M. Castello, G. Tortarolo, M. Buttafava *et al.*, "A robust and versatile platform for image scanning microscopy enabling super-resolution FLIM," *Nat. Methods* **16**(2), 175–178 (2019).

25. K. Zhao, X. Xu, W. Ren *et al.*, "Two-photon MINFLUX with doubled localization precision," *eLight* **2**, 5 (2022).

26. M. Weber, M. Leutenegger, S. Stoldt *et al.*, "MINSTED fluorescence localization and nanoscopy," *Nat. Photon.* **15**(5), 361–366 (2021).

27. M. Weber, H. Emde, M. Leutenegger *et al.*, "MINSTED nanoscopy enters the Ångström localization range," bioRxiv (2022).

28. C. P. Grabner, I. Jansen, J. Neef *et al.*, "Resolving the molecular architecture of the photoreceptor active zone by MINFLUX nanoscopy," bioRxiv (2021).

29. F. G. Ttfert, C. Wurm, V. Mueller *et al.*, "Coaligned dual-channel STED nanoscopy and molecular diffusion analysis at 20 nm resolution," *Biophys. J.* **105**(1), L01–L03 (2013).

30. T. Stephan, C. Brüser, M. Deckers *et al.*, "MICOS assembly controls mitochondrial inner membrane remodeling and crista junction redistribution to mediate cristae formation," *Embo. J.* **39**(14), e104105 (2020).

31. A. Lampe, V. Haucke, S. J. Sigrist *et al.*, "Multicolour direct STORM with red emitting carbocyanines," *Biol. Cell* **104**(4), 229–237 (2012).

32. H. Takakura, Y. Zhang, R. S. Erdmann *et al.*, "Long time-lapse nanoscopy with spontaneously blinking membrane probes," *Nat. Biotechnol.* **35**, 773–780 (2017).

33. P. J. Macdolnald, S. Gayda, R. A. Haack *et al.*, "Rhodamine-Derived Fluorescent Dye with Inherent Blinking Behavior for Super-Resolution Imaging," *Anal. Chem.* **90**(15), 9165 (2018).

34. S. Uno, M. Kamiya, T. Yoshihara, K. Sugawara *et al.*, "A spontaneously blinking fluorophore based on intramolecular spirocyclization for live-cell super-resolution imaging," *Nat. Chem.* **6**, 681–689 (2014).

35. S. Uno, M. Kamiya, A. Morozumi *et al.*, "A green-light-emitting, spontaneously blinking fluorophore based on intramolecular spirocyclization for dual-colour super-resolution imaging," *Chem. Sci.* **54**, 102 (2018).

36. R. Gerasimaite, J. Bucevicius, K. A. Kiszka *et al.*, "Blinking Fluorescent Probes for Tubulin Nanoscopy in Living and Fixed Cells," bioRxiv (2021).

37. Richard Lincoln, Mariano L. Bossi, Michael Remmel *et al.*," A general design of caging-group-free photoactivatable fluorophores for live-cell nanoscopy," *Nat. Chem.* (2022), https://doi.org/10.1038/s41557-022-00995-0.

38. M. Nirmal, B. O. Dabbousi, M. G. Bawendi *et al.*, "Fluorescence intermittency in single cadmium selenide nanocrystals," *Nature* **383**, 802–804 (1996).

39. C. Galland, Y. Ghosh, A. Steinbruck *et al.*, "Two types of luminescence blinking revealed by spectroelectrochemistry of single quantum dots," *Nature* **479**, 203–207 (2011).

40. B. Li, X. Y. Miao, Photoluminescence blinking properties of single $CsPbBr_3$ perovskite quantum dots, *Acta Phys. Sin.* **70**(20), 207802 (2021).

41. H. He, X. Liu, S. Li *et al.*, "High-density super-resolution localization imaging with blinking carbon dots," *Anal. Chem.* **89**(21), 11831–11838 (2017).

42. A. Szymborska, A. D. Marco, N. Daigle *et al.*, "Nuclear pore scaffold structure analyzed by superresolution microscopy and particle averaging," *Science* **341**(6146), 655–658 (2013).

43. K. Schücker, T. Holm, C. Franke *et al.*, "Elucidation of synaptonemal complex organization by superresolution imaging with isotropic resolution," *Proc. Natl. Acad. Sci. USA* **112**(7), 2029–2033 (2015).

44. J. M. Fritschy, "Is my antibody-staining specific? How to deal with pitfalls of immunohistochemistry," *Eur. J. Neurosci.* **28**(12), 2365–2370 (2008).

45. D. M. Chudakov, M. V. Matz, S. Lukyanov *et al.*, "Fluorescent proteins and their applications in imaging living cells and tissues," *Physiol. Rev.* **90**(3), 1103–63 (2010).

46. S. Wang, J. R. Moffitt, G. T. Dempsey *et al.*, "Characterization and development of photoactivatable fluorescent proteins for single-molecule-based superresolution imaging," *Proc. Natl. Acad. Sci. USA* **111**(23), 8452–8457 (2014).

47. J. Q. Wu, T. D. Pollard, "Counting cytokinesis proteins globally and locally in fission yeast," *Science* **310**, 310–314 (2005).

48. A. Keppler, S. Gendreizig, T. Gronemeyer *et al.*, "A general method for the covalent labeling of fusion proteins with small molecules in vivo," *Nat. Biotechnol.* **21**, 86–89 (2003).

49. G. V. Los, L. P. Encell, M. G. Mcdougall *et al.*, "HaloTag: A novel protein labeling technology for cell imaging and protein analysis," *ACS Chem. Biol.* **3**, 373–382 (2008).

50. S. J. Sahl, S. W. Hell, S. Jakobs *et al.*, "Fluorescence nanoscopy in cell biology," *Nat. Rev. Mol. Cell. Biol.* **18**, 685–701 (2017).

51. H. Li, J. C. Vaughan, "Switchable fluorophores for single-molecule localization microscopy," *Chem. Rev.* **118**(18), 9412–9454 (2018).

52. L. Arrico, L. D. Bari, F. Zinna, "Quantifying the overall efficiency of circularly polarized emitters," *Chem. Eur. J.* **27**, 2920 (2021).